Journal of *Marine Science and Engineering*

MDPI

Article

Environmental Impact of Irgarol 1051, a Biocide, on Marine Microalgae Metabolism: A Case Study of *Chlorella salina* and *Dunaliella bardawil*

Mona I. A. Kaamoush [1], Antonio Scopa [2,*], Marios Drosos [2] and Ahmed M. El-Zeiny [3,*]

[1] Environmental Protection and Crises Management Department, Simulators Complex, Arab Academy for Science, Technology and Maritime Transport (AAST), Alexandria 1029, Egypt; monakaamoush@aast.edu
[2] School of Agricultural, Forest, Food, and Environmental Sciences (SAFE), University of Basilicata, Via dell'Ateneo Lucano 10, 85100 Potenza, Italy; marios.drosos@unibas.it
[3] Environmental Studies Department, National Authority for Remote Sensing and Space Sciences (NARSS), Cairo 11769, Egypt
* Correspondence: antonio.scopa@unibas.it (A.S.); aelzeny@narss.sci.eg (A.M.E.-Z.); Tel.: +20-1007737052 (A.M.E.-Z.)

Abstract: Preventing fouling is crucial for maintaining ship performance, as it reduces speed, increases fuel consumption, raises greenhouse gas emissions, and spreads invasive species. Irgarol 1051, an antifouling agent (2, methythiol-4, tert-butylamino, 6-cyclopropylamino, s-triazine), is a toxic compound that impacts various marine species. It inhibits algal growth and disrupts key metabolites, posing a threat to the marine ecosystem. This study aimed to assess the toxic effects of Irgarol 1051 on *Chlorella salina* and *Dunaliella bardawil*, two nutrient-rich marine algae commonly used in fish feed. In addition, the suitability of the Mediterranean Sea coast for algal proliferation was assessed using geospatial techniques. The data were statistically examined using a two-way ANOVA test. Lethal and sublethal effects of Irgarol 1051 were measured in the laboratory to identify the consequences of this biocide on certain metabolite compositions. EC50 for *C. salina* and *D. bardawil* was estimated to be 0.50 $\mu g \cdot L^{-1}$ and 0.025 $\mu g \cdot L^{-1}$ respectively. IR spectroscopy of total cell constituents, protein profile, and the damaging effects of antioxidants have been evaluated for the two algal species. The findings of this study revealed that Irgarol 1051 negatively affected all the examined metabolites in both algal species, with more pronounced impacts on the wall-less alga *Dunaliella bardawil* compared to the walled alga *Chlorella salina*. A notable increase in total antioxidants was observed in both algae as the Irgarol concentration increased. The study reveals high algal growth areas near the Nile Delta along the Egyptian coast, potentially vulnerable to the effects of Irgarol 1051 due to nutrient runoff and eutrophication. The spatial analyses showed that the growth of *C. saline* and *D. bardawil* in Egyptian seawater is high in front of the Nile delta governorates: Port Said, Damietta, and Dakhalia shores reporting 6, 4.5, and 4 $mg \cdot m^{-3}$, respectively. The level of mass chlorophyll "a" in front of the Egyptian northern governorates can be ordered as follows: Port Said > Damietta > Dakahlia > North Sinia > Kafr El-Sheikh > Alexandria > Matrouh. This study highlights the use of spatial analyses to assess algal distribution, pollution impact, and ecosystem vulnerability along the Egyptian Mediterranean coast for effective environmental management.

Keywords: antifouling; Irgarol 1051; marine algae; IR spectroscopy; spatial analyses; Egyptian coastal water; protein profiles; antioxidants

Academic Editors: Ali Parsaeimehr and Gulnihal Ozbay

Received: 15 February 2025
Revised: 27 March 2025
Accepted: 28 March 2025
Published: 30 March 2025

Citation: Kaamoush, M.I.A.; Scopa, A.; Drosos, M.; El-Zeiny, A.M. Environmental Impact of Irgarol 1051, a Biocide, on Marine Microalgae Metabolism: A Case Study of *Chlorella salina* and *Dunaliella bardawil*. *J. Mar. Sci. Eng.* **2025**, *13*, 695. https://doi.org/10.3390/jmse13040695

1. Introduction

Biofouling on submerged maritime structures can lead to increased fuel consumption, higher frictional resistance, reduced maneuverability, and greater maintenance and cleaning costs [1]. Marine pollution caused by antifouling substances is now regarded as one of the world's most serious problems. As a result, scientists and environmentalists are increasingly concerned about the environmental degradation caused by these chemicals [2]. Marine constructions frequently use antifouling paint to prevent biofouling. By 2021, the market of antifouling coatings and paints is expected to be valued at USD 9.22 billion [3]. In the coming years, the global market for antifouling coatings is anticipated to increase significantly. As indicated by a report published in November 2024, the market is projected to develop at a compound annual growth rate (CAGR) of 8.2% from 2024 to 2030, reaching a size of USD 16.40 billion [4]. As mentioned by a report published in October 2024, the market is expected to grow at a compound annual growth rate (CAGR) of 8.22% from 2024 to 2034, surpassing USD 22.68 billion. According to these forecasts, the antifouling coatings market is expected to grow steadily due to rising demand for these products in a variety of applications [5].

The practice of antifouling for boats and ships dates back to ancient Greek and Roman times. Early antifouling coatings, including grease, tar, brimstone, and sulfur pitch, were later developed in the United Kingdom. Irgarol 1051 on the French Riviera was the first known instance of booster biocides contaminating waters near the coast [6]. To combat iron ship corrosion, copper sheathing—used over a century ago—prevented fouling by releasing toxic metal ions. This innovation eventually led to the development of antifouling coatings in the mid-1800s [7,8]. Despite recent legislative changes, copper oxide has been the most widely used antifouling agent in the UK for the past ten years, following in sequence of application by TBT, Irgarol 1051, diuron, dichlofluanid, and zinc [9].

Significant levels (till 1700 ng per liter) were identified in the nearby marinas. Several antifouling substances (biocides), that are found in high boating activity regions, exist in combination form [10]. Irgarol 1051 was discovered in 13 of 26 saltwater samples collected from various marine areas, making it the most frequently occurring antifouling component. The highest ever measured concentration was 4.0 μg L^{-1}. It was discovered to indicate ecological risk from strains in the Arctic [11].

Following a restriction on tributyle-tin (TBT) use due to its negative environmental effects, Irgarol 1051 became the most well-known biocide. This resulted in a revenue loss of USD 147 million in the Arcachon Bay area [12]. At low concentrations (up to 10 ng/L), it was also discovered that other mollusk types' wild populations were impacted [13]. The European Community, in 1989, implemented a regulation that prohibited the application of tributyle-tin on ships shorter than 25 m [14].

As the principal producers in aquatic ecosystems, algae are essential. It is believed that half of the world's primary production, which provides the minerals and energy needed to maintain planetary ecosystems, is produced by algae and cyanobacteria [15]. The origins of microalgae vary according to species, size, and the structure of the cell wall, as well as the many enzymes that break them down. These species also range in terms of how sensitive and reactive they are to organotin chemicals. As a result, several species have been observed to develop tolerance to organotin chemicals, either breaking them down or accumulating them [16].

Irgarol 1051 is a diamino-1,3,5-triazine that is 1,3,5-triazine-2,4-diamine carrying a N-tert-butyl, N′-cyclopropyl, and a methyl-sulfanyl group at position 6. It has a role as an antifouling biocide, a xenobiotic, and an environmental contaminant. It is an aryl sulfide, a member of cyclopropanes, and a diamino-1,3,5-triazine. It is functionally related to a 1,3,5-triazine-2,4-diamine. It derives from a hydride of 1,3,5-triazine (source: National Library

of Medicine). There are structural similarities between Irgarol 1051 and other s-triazine derivatives like simazine and atrazine. Among the main functional groups of Irgarol are the methylthio group, alkylamino substituents, and the s-triazine core, which all work together to effectively block photosystem II (PSII) in aquatic plants and algae. Atrazine and simazine both function as PSII inhibitors and share this mechanism. However, unlike atrazine, Irgarol is more hydrophobic, preventing the attraction of freshwater and marine algae. Irgarol 1051, an s-triazine-based herbicide, is frequently used in European coastal waters. Additionally, it has been demonstrated that Irgarol 1051 is extremely harmful to freshwater and marine microalgal growth and also to the initial phases of macroalgae zoospore formation [17]. For instance, at sub-nanomolar dosages, Irgarol has an impact on the algal population [18]. Irgarol 1051 is very detrimental to aquatic life, especially primary producers, because it suppresses PS II [19]. Antifouling Irgarol showed a highly destructive impact on different marine algae—especially in ports with high shipping activities—due to its high concentrations in marine ports. It showed highly adverse effects on the growth, amino acids, and total chlorophyll content of different marine algae [7,11].

The monitoring study by Muñoz et al. [20] on Irgarol toxicity among 12 mico-organic pollutants on Spain's beach showed that antifouling Irgarol exceeds the adverse effect threshold for marine species. The average concentration of Irgarol in Spain's beach was around 0.36 ng·L^{-1}. However, studies have shown that this compound has a modest potential for bioconcentration, posing minimal risk to humans and predators consuming fish. On the other hand, Cima and Varello [21] demonstrated that Irgarol exhibits toxicity to animals. Given its widespread use in the marine environment for many years, there is an undeniable risk to coastal biocoenoses due to chemical interactions between Irgarol and various ligands, complex formation, and bioaccumulation within trophic chains. Paints often contain Irgarol, an antifouling chemical, to stop fouling organisms from attaching to and growing on ship hulls or other underwater structures. Worldwide limitations on incorporating them in antifouling paints have been brought by worries about their toxicity to aquatic creatures that are not intended targets [22].

It is common for organisms in high-shipment marine environments to be simultaneously exposed to a range of biocides that have the ability to interact and affect vulnerable species in an antagonistic, additive, or synergistic manner [23]. The European Union created the Biocidal Agents Directive to permit the use of biocidal chemicals inside its boundaries. The unified data standards have been used by the EU for both new and ongoing biocide programs. Each antifouling agent submitted for registration was required to provide a baseline set of data [24]. The prohibition on the use of antifouling systems containing Irgarol-1051 officially came into effect on 1 January 2023 [25].

Due to the synergy between various nutrients and antioxidant components, the two marine algae species in this study possess an excellent nutritional profile. Unlike many plant-based food sources, they provide essential nutrients, proteins, and vitamins, including vitamin D and B12. In contrast, *chlorella* products offer these elements and more. Compared to other plant-based diets, *Chlorella* sp. has higher levels of iron and folate Aquaculture can safely and sustainably use *Chlorella* sp. as it does not contain any hazardous compounds [26,27]. Due to the high concentration of vital amino acids, protein, fats, carbs, vitamins, and pigments found in *Dunaliella* sp., it is recommended that fish use this natural feed. It is said to be abundant in beneficial antioxidants such as vitamin B_{12}, β-carotene, zeaxanthin, and omega-3 polyunsaturated fatty acids [28].

The purpose of the work was to assess the harmful effects of Irgarol 1051, a biocide frequently found in antifouling systems, against two marine algae species: *Dunaliella bardawil* and *Chlorella salina*. The objective of the study was to investigate how Irgarol 1051 affected algal growth and metabolite composition in a lethal and sublethal impact.

In order to accomplish this, comprehensive analyses, including IR spectroscopy, protein profiling, and evaluations of antioxidant activity, and the employed laboratory tests have been carried out to determine the concentration at which 50% of algae were affected (EC50). Additionally, the study used spatial analysis to monitor the proliferation of algae in Egyptian coastal waters in order to pinpoint areas where these algae are most prevalent, especially in front of the governorates of the Nile Delta.

Spatial analysis plays a vital role in mapping the distribution of *Dunaliella bardawil* and *Chlorella salina* along the Egyptian Mediterranean coast. Using remote sensing, GIS, and other spatial tools, researchers can monitor the proliferation of these algae, identify high-density zones, and analyze environmental factors influencing their growth. This approach helps pinpoint optimal locations for potential commercial cultivation, assess ecological impacts, and track seasonal variations. In regions like the Nile Delta, where coastal conditions fluctuate, spatial analysis provides valuable data for sustainable management and conservation efforts.

2. Materials and Methods

2.1. Algal Growth and Experiments Planning

The two algae used in this research, *Chlorella salina* and *Dunaliella bardawil*, were provided as gifts from the Algal Collection Laboratory, Faculty of Science, Alexandria University. The origins of these algal species are described as follows:

Chlorella salina has been obtained from UTEX—the culture collection of algae, Texas University, Austin, TX, USA. Taxonomy ID: 289237, CCAP 211/25. *C. salina* is a green, unicellular alga that is highly adaptable to a wide range of salinity levels and typically measures between 2 and 10 μm in diameter.

The *Dunaliella bardawil* strain, designated as "UTEX 2538" in the UTEX Culture Collection of Algae, was originally isolated from the Bardawil Lagoon in North Sinai, Egypt. The basal media used for cultivating both algae in this study followed the methodology described by Boussiba et al. [29]. *D. bardawil* is a unicellular green alga capable of withstanding high salt exposure, measuring 5–9 μm in width and 7–12 μm in length, and lacking a rigid cell wall.

Two algae species were grown under ideal circumstances (temperature at 28 °C ± 3 °C and light at 80 lux). A batch culture system was used to perform the toxicity experiments in a controlled culturing chamber. Under a 12 h light/12 h dark photoperiod, the cultures were kept in order to simulate the normal diurnal cycles. The formula of Robert [30] was applied to estimate the rate of growth (number of divisions in a day) using Perkin Elmer (Lambada 1) ultra violet spectrophotometer. Three replicates were performed for each part of the assays.

$$R = (3.322/(t_2 - t_1) \times (\log N_2/N_1).$$

where 3.322: constant of growth. t_1 = the experiment's start time; t_2 = The experiment's end time; N_1 = Number of cells per ml culture at t_1; and N_2 = Number of cells per ml culture at t_2.

Herbicide (Irgarol 1051) provided by Fluka Co. Egypt (21 Elfardous St, Abbassya Cairo, Egypt 11381). A total of 100 mL acetone was used to dissolve 1000 mg of Irgarol, and the stock solution was stored and kept in the dark at 4 °C. A total of 100 milliliters of sterilized distilled water was mixed with 0.1 milliliters of stock solution. Each microalgae medium was combined and diluted with this stock solution. A one-liter medium was mixed with various concentrations that were created (primarily, experiments were conducted on the effect of Irgarol on the growth of the two studied organisms in order to select a suitable concentration). Initially, both organisms perished under all the tested concentrations of 300,

200, 150, and 100 $\mu g \cdot L^{-1}$. This study aimed to determine the optimal concentrations for the growth of the marine unicellular green algae *Chlorella salina* and *Dunaliella bardawil*.

2.2. Infrared Spectra

Preliminary testing established the optimal cell suspension density needed to generate spectra with a strong signal. According to the procedures of Kansiz et al. [31], Lugol's iodine liquid was employed to make pellets with a specific volume of algae culture. The dried microorganisms were placed on an infrared microscope phase to collect spectrum data for an IR study. Perkin Elmer 1430 ratio recorder, an infrared spectrophotometer, was used for acquiring the spectra. The absorbance spectra were generated by combining ten images and averaging them, covering a wavelength range of 4000 to 500 cm^{-1}.

2.3. Protein Profile Analyses

The protein profile was examined using Gianazza et al. [32] procedure, using phase-system equipment for polyacrylamide gel electrophoresis using sodium dodecyl sulfate (SDS-PAGE). The samples were blended together using 5 mL of pH 7.2 tris-HCl buffer. After centrifuging the homogenate solution for ten min at 6000$\times$ *g*, the transparent supernatant was promptly checked. Sampling and molecular weight indicators (BioRad, pertained SDS markers) were added to the slab gel. For almost two hours, the electrophoresis process was run at a constant 150 V voltage. This gel was dyed via Coomassie Brilliant Blue R-250 (0.06% Coomassie Brilliant Blue R-250 in 50% methanol and 10% acetic acid) for 60 min at ambient temperature while gently stirring.

2.4. Total Antioxidants

In line with Azizullah's [33] method for separating H_2O_2, 0.5 g fresh alga was homogenized in 5 mL of ice-cold trichloroacetic acid (TCA) to evaluate hydrogen peroxide. After 10 min of centrifugation at 12,000$\times$ *g*, 1.5 mL of potassium phosphate buffer (50 mM, pH 7.0) was added to 0.5 mL of the supernatant and 1 mL of 1 M potassium iodide (KI). The reaction mixture was kept for one hour at room temperature in the absence of light. Thus, the absorbance is measured at A_{390} nm.

2.5. Potential of Algae Growth Along the Egyptian Mediterranean Coast

In the present study, geospatial techniques were used to assess and map the potential sites of *Dunaliella bardawil* and *Chlorella salina* on the Egyptian Mediterranean Coast. The Copernicus marine data were used for retrieval of mass concentration of chlorophyll-a in the seawater during the year 2024 to assess the potential sites for algae along the Mediterranean coast. The Copernicus system generates 10-day global ocean forecasts at a 1/4-degree resolution, updated weekly. It compiles a rolling two-year time series, providing daily and monthly averages of biogeochemical parameters like chlorophyll-a concentration ($mg \cdot m^{-3}$). The data are presented globally with a 1/4-degree horizontal resolution using a regular longitude/latitude equirectangular projection, supporting both temporal and spatial oceanographic analysis. The resolution of the resultant map was improved using ArcGIS 10.8 using the geostatistical analyses.

2.6. Statistical Analysis

Two-way ANOVA (Analysis of Variance) was used to statistically analyze the data. The difference between the mean probability values was examined using Duncan's New Multiple Range Test (p 0.05). LSD (Least Significant Difference), set at 0.05, was also ascertained using the F test.

3. Results and Discussion

On the Mediterranean coast of Egypt, the mass concentration of algae, which is represented by chlorophyll, varied from east to west. Using geostatistical studies and remote sensing, we examined the possible locations for algal development throughout the Mediterranean coast of Egypt. The two tested algal species" *Chlorella salina* and *Dunaliella bardawil* "were significantly inhibited at all the tested Irgarol doses, which correlated with the biocide's increasing toxicity.

To determine the effective concentration (EC_{50}) of Irgarol 1051 for *Chlorella salina* and *Dunaliella bardawil*, the organisms were cultured under varying concentrations of the compound. The results indicated that both algae perished within two days of exposure. *Dunaliella bardawil* exhibited more severe adverse effects compared to *Chlorella salina*. Experiments conducted under different concentrations revealed that both organisms experienced significant stress and perished by the sixth day. The effective concentration (EC_{50}) for *C. salina* was approximately 0.5 $\mu g \cdot L^{-1}$ on the eighth day, whereas for *D. bardawil*, it was much lower at 0.025 $\mu g \cdot L^{-1}$. These results indicate that D. bardawil is more sensitive to Irgarol 1051 than C. salina. The tested Irgarol 1051 doses for *C. salina* were 0.25, 0.5, and 0.75 $\mu g\ L^{-1}$, while for *D. bardawil* they were 0.012, 0.025, and 0.05 $\mu g\ L^{-1}$ (one higher and one lower dose for each algal species).

The results presented in Figure 1 and Supplementary Materials Table S1 indicate that algal growth steadily increased until the eighth day for both organisms, reaching its peak compared to the controls. However, the growth rates varied depending on the Irgarol concentration, with *Dunaliella bardawil* experiencing greater growth inhibition than *Chlorella salina*.

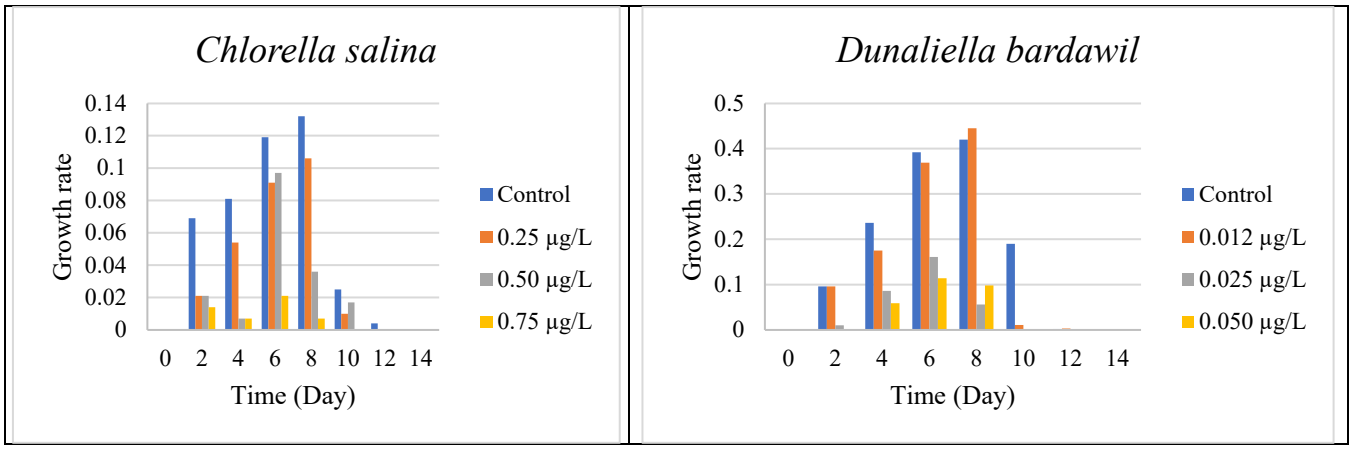

Figure 1. Growth rates of *C. salina* and *D. bardawil* in response to varying Irgarol 1051 concentrations.

A two-way ANOVA test was used to determine the effect of Irgarol 1051 on the growth of *Chlorella salina* and *Dunaliella bardawil* during the 14 days. The study found a dose-dependent decrease in algal growth, with higher levels of Irgarol 1051 causing stronger growth inhibition ($p < 0.01$). Least Significant Difference (LSD) testing revealed significant differences between the control and treatment groups. The impact was more evident in *D. bardawil*, indicating a greater sensitivity to the biocide than *Chlorella salina.*

However, Gatidou et al. [34] observed that Irgarol 1051 inhibits the growth of *Dunaliella tertiolecta* at concentrations greater than 0.8 $\mu g \cdot L^{-1}$ and kills almost all of the cells at 3.0 $\mu g \cdot L^{-1}$. Similarly, Kaamoush and El-Agawany [35] reported comparable findings, indicating that Dunaliella salina exhibited growth stimulation at the lowest concentration of the antifouling agent Irgarol (0.012 $\mu g \cdot L^{-1}$). However, as the Irgarol concentration increased, a progressive inhibition in growth was observed. The findings obtained are

in line with those explained by Anita et al. [36] who demonstrated that at doses below 100 ng L^{-1}, Irgarol kills 50% of the phytoplankton. It has been demonstrated that Irgarol 1051 is an acutely dangerous chemical for cyanobacterial growth since it inhibits cell growth at doses ranging from 5 to 10 µg·L^{-1} at 4 days [33–37].

3.1. Infrared Spectroscopy

IR spectroscopy enables rapid examination with tiny quantities of material while providing good analytical quality. It provides a signature of the macromolecular makeup of the cells. Chemometrics has advanced to the point where it is possible to quantify not just large cellular pools like protein, lipid, and carbohydrate but also small components to consider. Table 1 records the obtained infrared spectra of the investigated two algae, *C. salina* and *D. bardawil*, which were cultivated for 8 days while being treated with Irgarol 1051, an antifouling agent. Figure 2 shows the graphs of these spectra. The entire biochemical makeup of the algae cells was represented in these data. These displayed the band assignments that were derived from analyses of macromolecules and whole cell organelles in the 4250–500 cm^{-1} range. The overall count of spectrum ranges that are able to explain the chemical standards of the two examined algae at the regions between 4250 and 500 cm^{-1} was indicated by the obtained spectra.

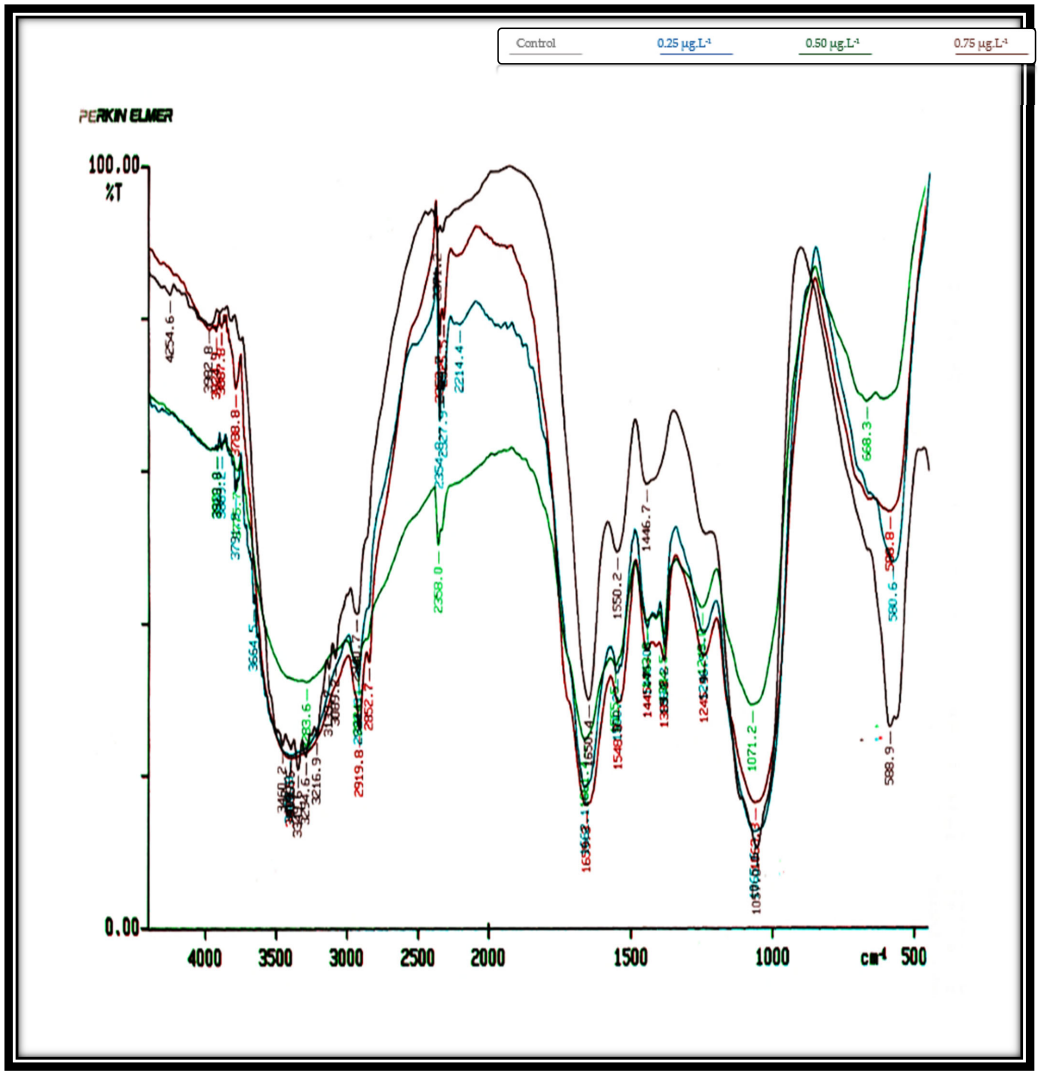

Figure 2. Effect of varying Irgarol 1051 concentrations (control, 0.25 µg·L^{-1}, 0.50 µg·L^{-1}, and 0.75 µg·L^{-1}) on the infrared spectroscopy of *C. salina* on the 8th day of culturing.

Table 1. Effect of varying Irgarol 1051 concentrations on the number of peaks of the infrared spectroscopy of *C. salina* cultured for 8 days.

Frequency	Control	0.25 μg·L^{-1}			0.50 μg·L^{-1}			0.75 μg·L^{-1}			ANOVA *p*-Value
		Present	Absent	New	Present	Absent	New	Present	Absent	New	
4250–3500	2	4	-	2	3	-	1	2	-	-	$p < 0.05$
3500–2750	8	2	6	-	3	5	-	2	6	-	$p < 0.01$
2750–1750	1	3	-	2	2	-	1	1	-	-	$p = 0.07$
1750–1060	3	5	-	2	5	-	2	5	-	2	$p = 0.15$
1060–500	2	2	-	-	2	-	-	2	-	-	Not significant
Total	16	16	6	6	15	5	4	12	6	2	

The IR spectra of untreated (control) *Chlorella salina* cells displayed a total of 16 peaks. At Irgarol concentrations of 0.25, 0.50, and 0.75 μg·L^{-1}, the analysis revealed the presence of 16, 15, and 12 peaks, respectively. The majority of the peaks are found between 3500 and 2750 cm^{-1} in frequency. While the majority of the peaks in the treated cultures were observed at frequencies between 1750 and 1060 cm^{-1} (five peaks), the control culture had eight peaks. In the frequency range of 3500–2750 cm^{-1}, the control culture exhibited eight peaks. However, at the same frequencies, only six peaks were observed in cultures treated with Irgarol at concentrations of 0.25, 0.50, and 0.75 μg·L^{-1}, respectively. Furthermore, Table 1 data clearly shows that six new peaks occurred at concentrations of 0.25 μg·L^{-1} and 0.50 μg·L^{-1} of Irgarol, four new peaks appeared at Irgarol concentrations ranging from 0.50 μg·L^{-1} to 0.75 μg·L^{-1}, with only two new peaks detected.

Methyl group, methylene group, and methyl group Vas C-H are represented by the eight number of peaks that emerged in the 3500–2750 cm^{-1} control zone, mostly from lipids and fatty acids, in combination with V C=O of ester functional groups [38]. The spectral bands ranging from 1153~1020 cm^{-1} may be definitively attributed to carbohydrates, mostly because of C-O-C stretching vibrations. However, there is a band at 1080 cm^{-1} that also includes contributions from phosphorylated compounds including nucleic acids and carbohydrates [39]. In the treated cultures, most of these significant chemical compounds disappeared. However, in *Chlorella salina*, no noticeable effect was observed for molecules within the frequency range of 1060–500 cm^{-1}, which corresponds to the N, C, O, and H bonds of polysaccharides. The asymmetric stretching mode of phosphorylated molecules, including nucleic acids, and the contributions from carbohydrates are shown by the band at 1080 cm^{-1} [40].

At frequencies between 1750 and 1060 cm^{-1}, an equal number of peaks (5) appeared across all the treated concentrations of Irgarol 1051. This suggests that two new compounds emerged at these frequencies in all the treated samples compared to the control. These peaks correspond to amides associated with proteins and the phosphodiester backbone of DNA and RNA. Additionally, bands arising from P=O asymmetric stretching or C-H ring bending provided further structural information [41]. Under these frequencies, two bands appeared new under all the tested concentrations of Irgarol.

At frequencies 2750 to 1060 cm^{-1}, the total peaks at control were four: eight at 0.25 μg·L^{-1}, seven at 0.50 μg·L^{-1}, and six at 0.75 g/L Irgarol 1051. These findings demonstrate that the majority of the novel compounds discovered at these frequencies are amides connected with protein, as well as ether functional groups from lipids and fatty acids [42]. This phenomenon is also related to neutral lipids' protective actions towards stresses [43].

Table 2, Figure 3 show the influence of concentrations of 0.012, 0.025, and 0.050 μg·L^{-1} Irgarol on *D. bardawil*'s IR spectra cell cultures for eight days. These findings indicate that *D. bardawil* was more severely affected by Irgarol toxicity than *C. salina*. In the untreated control culture, a total of 14 peaks were observed. However, as the concentration

of Irgarol increased, the number of peaks significantly decreased, indicating potential structural or biochemical alterations in the treated samples. As compared to the controlled culture, the total number of peaks at concentration 0.012 $\mu g \cdot L^{-1}$ Irgarol was eleven peaks, meaning that three peaks vanished. At concentration 0.025 $\mu g \cdot L^{-1}$ Irgarol, nine peaks appeared simultaneously, six peaks vanished, and only one peak appeared in the region of 1060–500 cm^{-1} (i.e., polysaccharides). At an Irgarol concentration of 0.050 $\mu g \cdot L^{-1}$, only seven peaks were visible, with seven peaks simultaneously disappearing. The majority of the vanished peaks were located between 4250 and 3500 cm^{-1} in frequency. This indicates that the phosphodiester backbone of the nucleic acids, the methyl and methylene groups, and the amides linked to proteins vanished. This could be the reason why *C. salina* is less sensitive to Irgarol 1051 than *D. bardawil*.

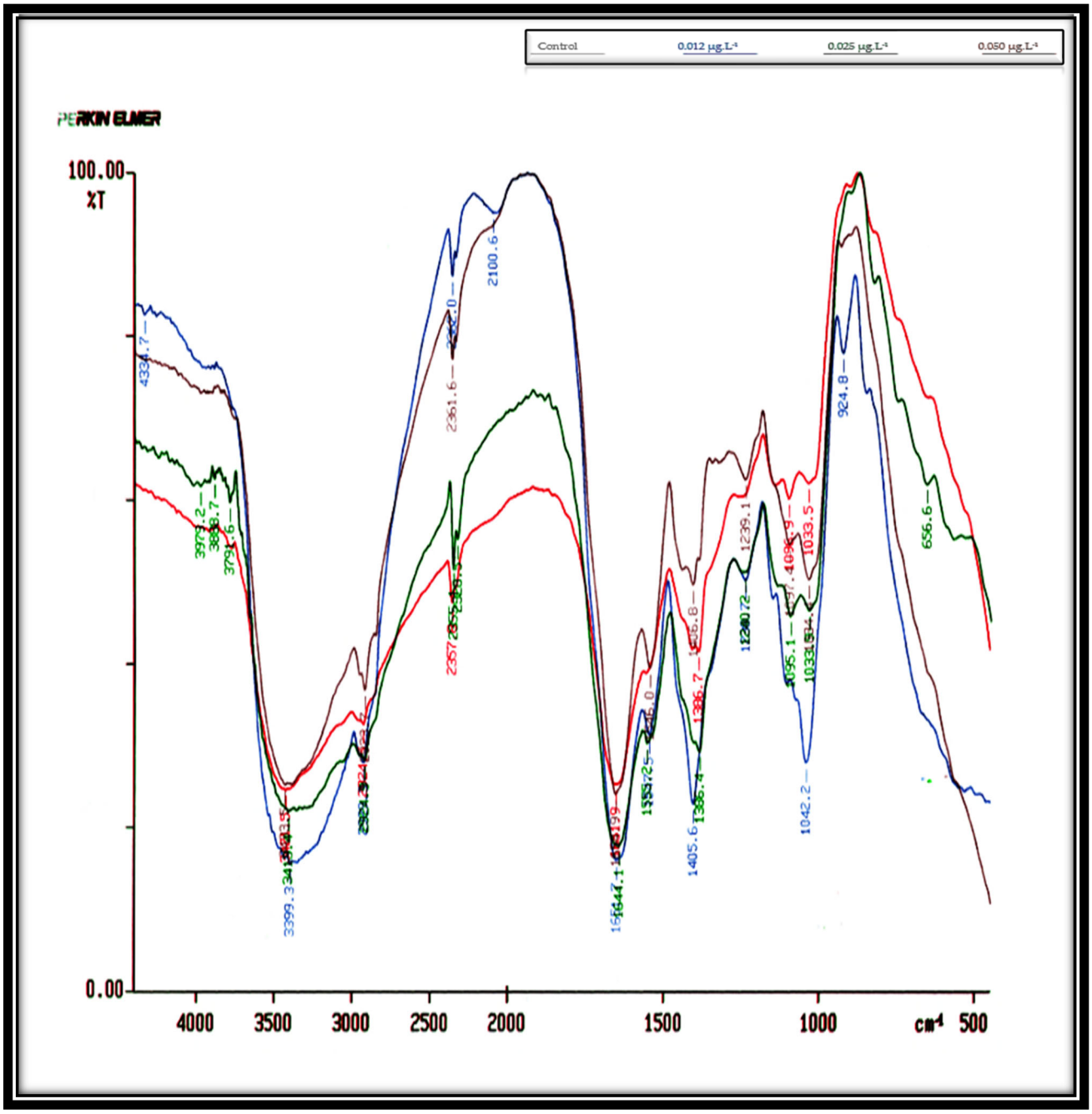

Figure 3. Effect of varying Irgarol 1051 concentrations (control, 0.012 $\mu g \cdot L^{-1}$, 0.025 $\mu g \cdot L^{-1}$, and 0.050 $\mu g \cdot L^{-1}$) on the infrared spectroscopy of *D. bardawil* on the 8th day of culturing.

Table 2. Effect of varying Irgarol 1051 concentrations on the number of peaks of the infrared spectroscopy of *D. bardawil* cultured for 8 days.

Frequency	Control	0.012 µg·L^{-1}			0.025 µg·L^{-1}			0.050 µg·L^{-1}			ANOVA *p*-Value
		Present	Absent	New	Present	Absent	New	Present	Absent	New	
4250–3500	3	1	2	-	-	3	-	-	3	-	$p < 0.01$
3500–2750	2	2	-	-	2	-	-	2	-	-	$p < 0.01$
2750–1750	2	2	-	-	1	1	-	1	1	-	$p = 0.04$
1750–1060	4	4	-	-	2	2	-	1	3	-	$p = 0.05$
1060–500	3	2	1	-	4	-	1	3	-	-	$p < 0.05$
Total	14	11	3	-	9	6	1	7	7	-	

A comparison with the control revealed that some peaks disappeared, new ones emerged, and others remained unchanged. The positions of some of the cell compounds' side chains may have changed, or some compounds with large molecular weights may have vanished in favor of compounds with lower molecular weights, explaining the development of new peaks under Irgarol stress. These findings align with those of Dao et al. (2017) [41], who observed that in the infrared (IR) spectra of *Chlorella* sp. and Scenedesmus acutus cultures treated with varying concentrations of Pb, there was a noticeable increase in lipids and carbohydrates, likely linked to detoxification mechanisms. Meanwhile, other components, such as proteins and phosphorylated molecules, showed a decrease. These latter effects were related to either the metal's direct effects on the synthesis/degradation of the algae or the indirect effects of produced ROS during Pb treatment. The results also match with the findings of El-Agawany and Kaamoush [44] who demonstrated that an infrared (IR) analysis of *Dunaliella tertiolecta* cultures treated with varying zinc concentrations revealed alterations in peak number and creation of different compounds. The frequencies 3500–2750 cm^{-1}, which correspond to the Vas C-H of methyl groups, Vas C-H of methylene groups, and Vas C-H of methylene groups, were the only ones that did not alter at any of the amounts examined [45], together with V C=O of ester functional groups, which are mostly derived from fatty acids and lipids [38]. These findings may demonstrate that the antifouling agent concentration and the type of organism are the primary determinants of the harmful effect of Irgarol. The emergence and disappearance of certain compounds were primarily influenced by factors such as the level of the stress agent, the slow synthesis rate of specific compounds, the positioning of certain side chains, the breakdown of complex molecules into simpler ones, and the type of organism under study [46,47].

In regard to statistical analysis, we have completed a thorough evaluation of the IR spectrum alterations using statistical comparisons. We assessed how Irgarol 1051 concentration and treatment time affected peak variations using a two-way ANOVA test. Both *C. salina* and *D. bardawil* showed statistically significant ($p < 0.05$) peak modifications (disappearance, appearance, or shift), according to the data. Our findings are supported by the statistical analysis, which shows that these spectrum alterations are a direct result of Irgarol exposure rather than being random.

3.2. Total Soluble Protein Profile Bands

Microalgae are regarded as significant supplies for the commercial production of protein because of their high protein content, so they are used as a particular fish meal in the aquaculture sector [48]. Proteins contain sequential copies of genetic information, translating nucleotide bases into long chains of amino acids. Comparing protein profiles allows for a clearer understanding of the differences and similarities between treated and untreated algae, helping to identify biochemical changes induced by treatment [49].

The total protein profile bands of untreated (control) and treated organisms under different concentrations of Irgarol 1051 were recorded in Supplementary Materials Tables S2–S4 for *Chlorella salina* and Supplementary Materials Tables S5–S7 for *Dunaliella bardawil*, as well as Supplementary Materials Figures S1–S3 for both algal species. These data show that some protein bands remained unaltered, while some looked new and others disappeared when compared to the control. Algae are found in a variety of environments, ranging from fresh water to a hypersaline water system. These organisms can normally survive in conditions with drastic changes in their surroundings. However, in response to the stress of these environments, changes in enzyme activity and thallus shape are common [50,51]. Consequently, modifications to these species' protein structures may also be connected to methods of adaptation. Stress-related symptoms of protein synthesis have been demonstrated in algae during this phase [52]. The findings showed that protein synthesis in response to stress in *C. salina* and *D. bardawil* indicated the presence of stress-specific proteins, influenced by certain environmental stress factors.

In the control culture of *Chlorella salina*, the total number of protein bands detectable on the gel plate was 12; however, in the treatment cultures, this number was reduced depending on the dose of Irgarol. The lower the number of bands in comparison to the control, the higher the concentration of Irgarol. It is also obvious from the data collected that the majority of the bands appeared in the range between 212 and 41 KDa. At 0.25 $\mu g \cdot L^{-1}$ concentration, there were nine bands overall, while at 0.75 $\mu g \cdot L^{-1}$ concentration, there were seven bands total. At concentrations of 0.25, 0.50, and 0.75 $\mu g \cdot L^{-1}$, the number of new bands in *C. salina* was three, four, and three. The disappearing bands, on the other hand, were six, six, and eight for concentrations of 0.25, 0.50, and 0.75 $\mu g \cdot L^{-1}$, respectively (Figures 4 and 5).

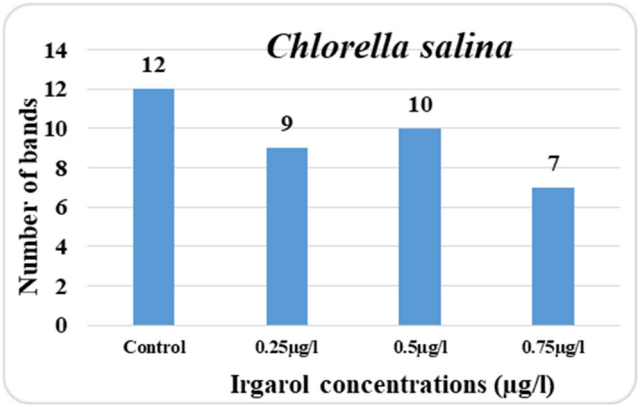

Figure 4. Effect of different Irgarol 1051 concentrations on total number of bands of protein profile in *Chlorella salina*.

Mohy El-Din and Abdel-Karee [49] observed that the greatest number of missing bands identified in the sea algae *C. salina* after copper and cadmium treatments was eight and five, respectively, which could be associated with DNA alterations. The total number of polymorphic bands in *C. salina* culture was 9, 10, and 11 with concentrations of 0.25, 0.50, and 0.75 $\mu g \cdot L^{-1}$, respectively, while the number of bands that stayed unaltered was 6, 6, and 4 at the same concentrations. Mohy El-Din et al. [53] reported that there were successive modifications to polymorphic bands and a decrease in protein fingerprinting in *Pterocladia capillacea* and *Ulva lactuca*, which could be the result of the presence of heavy metals having a deleterious effect on enzymes involved in protein production.

Ultimately, the percentage reduction in the total number of protein bands, compared to the control, was 25.0%, 16.67%, and 41.67%, respectively. On the other hand, there are now 9, 10, and 11 bands, respectively, more polymorphic bands. The number of unaltered

bands at concentrations of 0.75 μg·L^{-1}, 0.25, and 0.50 μg·L^{-1} was four, respectively. This could suggest that concentration 0.75 μg·L^{-1} is more hazardous than concentrations 0.25 and 0.50 μg·L^{-1}.

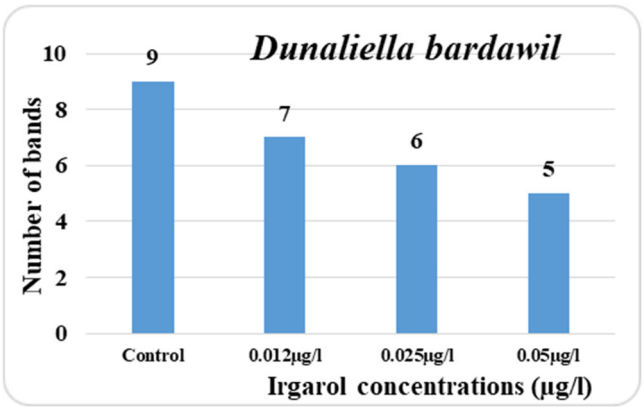

Figure 5. Effect of different concentrations of Irgarol 1051 on total number of bands of protein profile in *Dunaliella bardawil*.

The obtained data indicated that known antifouling Irgarol is more harmful to *D. bardawil* than *C. salina* as shown in Supplementary Materials Figures S1 and S2. While the doses of 0.012, 0.025, and 0.050 μg·L^{-1} produced seven, six, and five bands, respectively, the total number of bands in the untreated cultures (control) was nine. Among all the concentrations tested, only one band appeared as a new addition. In addition, the three distinct concentrations produced the appearance of two, three, and six more bands in comparison to the control. Additionally, the treatment concentrations had a significant impact on the polymorphic bands, which reached three, four, and seven in that order.

Eventually, the three tested concentrations of Irgarol each had an effect on four, two, and four bands, which remained unaffected. In comparison to the control, the percentage decrease in the number of bands was 22.2%, 33.3, and 44.4%, respectively. The data collected also clearly shows that in *D. bardawil*, the majority of the disappearing bands appeared in the low molecular weight region, and hence at the high Rf value region. Conversely, the majority of the unaltered bands were observed in the vicinity of low Rf values. The fact that *D. bardawil* is more susceptible to the antifouling Irgarol than *C. salina* may be explained by this map. El Taher [54] recognized that an organism's ability to survive under stressful conditions could be enhanced by the creation or accumulation of newly evolved proteins. Furthermore, Exss-Sonne et al. [55] came to the conclusion that the synthesis and build-up of novel proteins may enable algae to tolerate stress conditions. These findings are consistent with the observations for both kinds of algae. The results align with the findings of El-Agawany and Kaamoush [44], who stated that the stress effects of heavy metals on *Dunaliella tertiolecta* lead to biochemical modifications in certain molecules, particularly proteins.

Bands were dispersed throughout the gel plates in the total soluble protein profile for the two treated organisms and the control at the three varied Irgarol doses. The two studied organisms had different sums of all the bands that emerged on the gel plates, indicating that the number of bands depends primarily on the species and concentration of the stressing substance. However, it came to light through Sinha and Hader [56] that *Anabaena* sp. cultured under stressful conditions did not exhibit any alterations in their protein pattern. In contrast, numerous authors have noted that there was a noticeable alteration in the protein bands' composition under stress [57]. Additionally, El-Agawany et al. [58] observed that two additional appeared bands in *Spirulina platensis* cultivated under stress that were absent from the unaltered culture. Salah El-Din's [59] findings

demonstrated that the majority of algae species share physiological processes related to the production or biodegradation of certain macromolecules. The different variations in total soluble protein bands in stressed algae appear to be explained by this finding. According to Exss-Sonne et al. and Ahmed, 2010 [55,60], the organism can develop new protein production or accumulation to increase its stress tolerance. These findings are almost in agreement with those of *C. salina* and *D. bardawil.* The antifouling chemical Irgarol 1051 had a more deleterious impact on the protein profile in the wall-less alga *D. bardawil* than in the walled alga *C. salina*.

3.3. Activity of Total Antioxidants

Aerobic metabolism continuously generates reactive oxygen species (ROS), which are unstable free radicals that can damage lipids, proteins, and DNA. This oxidative stress contributes to cellular damage and plays a key role in the development of various diseases. Several types of photosynthetic cyanobacteria and green microalgae can produce antioxidants in response to oxidative stress induced by metals, acidity, pollution, ultraviolet radiation, and nutritional constraints [61].

Living organisms have developed an intricate antioxidant system in order to fend against ROS and minimize their damage. Enzymatic and non-enzymatic chemicals are included in these antioxidant systems. The total antioxidant activity of the system is represented by the sum of these antioxidants [47]. The collaboration of several antioxidants provides more protection versus bio-reactive oxygen damage than any single component alone. Thus, the total antioxidant capacity may provide more meaningful biological information than individual component measurements since it takes into account the overall impact of all antioxidants inside the organism's body cells [62].

Table 3 and Figures 6 and 7 present the results of the antioxidant capacity of *Chlorella salina* and *Dunaliella bardawil* at control and under different Irgarol 1051 concentrations. Reflecting on the study's findings regarding resistance, it is clear that species with greater stress tolerance often exhibit significantly higher antioxidant enzyme activity. The results showed that *C. salina* was more effective than *D. bardawil* at dissociating exogenous H_2O_2. The state of balance between the oxidative and antioxidative capacity determines the fate of the organism under oxidative stress. While Irgarol concentrations were 0.50 $\mu g \cdot L^{-1}$ for *C. salina* and 0.025 $\mu g \cdot L^{-1}$ for *D. bardawil*, there was a substantial increase in total antioxidant activity when compared to controls. The total antioxidants' activities are mostly determined by the stress impact, the period of cultivation, and the species evaluated [47].

Table 3. Antioxidant activity of *Chlorella salina* and *Dunaliella bardawil* examined at three different Irgarol 1051 concentrations on the 8th day of culturing.

Total Antioxidant Capacity (mM/L)			
Chlorella salina		***Dunaliella bardawil***	
Control	0.2 ± 0.40	Control	0.3 ± 0.11
0.25 $\mu g \cdot L^{-1}$	0.5 ± 0.57	0.012 $\mu g \cdot L^{-1}$	0.7 ± 0.06
0.50 $\mu g \cdot L^{-1}$	1.0 ± 0.60	0.025 $\mu g \cdot L^{-1}$	0.9 ± 0.75
0.75 $\mu g \cdot L^{-1}$	0.4 ± 0.90	0.050 $\mu g \cdot L^{-1}$	0.2 ± 0.86

In *C. salina*, total antioxidant activity increased by 2.5-, 5.0-, and 2.0-fold at Irgarol concentrations of 0.25, 0.50, and 0.75 $\mu g \cdot L^{-1}$, respectively, compared to the control. The outcomes achieved are very similar to those obtained by Ajitha et al. [63] who proved that exposure to zinc and mercury in *C. vulgaris* led to a notable increase in total antioxidant concentrations at baseline, which gradually decreased with acute and long-term exposure. Knauert and Knauer [64] supported the acquired outcomes, stating that intracellular ROS

accumulated in the microalgae *C. vulgaris* as a reaction to Cu toxicity. Consistent with the findings, *Anabaena doliolum* microalga cells have been shown to exhibit a similar trend in ROS formation in response to Zn^{2+}, achieving their maximal antioxidant doses greater than 0.7 mg·L^{-1} [65].

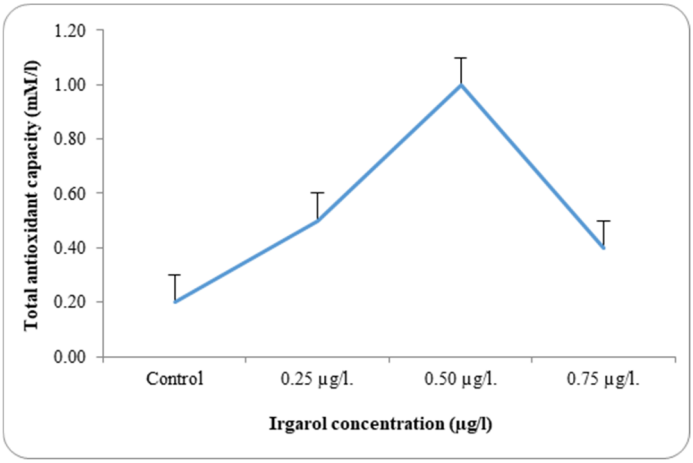

Figure 6. Antioxidant activity of *Chlorella salina* examined at three different Irgarol 1051 concentrations on the 8th day of culturing.

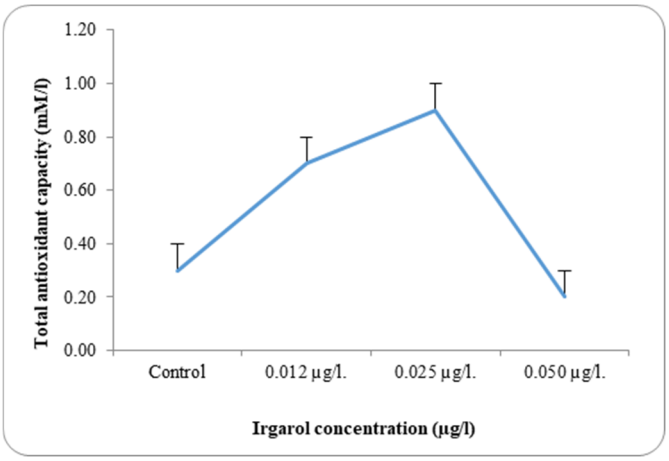

Figure 7. Antioxidant activity of *Dunaliella bardawil* examined at three different Irgarol 1051 concentrations on the 8th day of culturing.

In *C. salina*, total antioxidant activity decreased at an Irgarol concentration of 0.75 µg·L^{-1} but remained higher than under normal conditions (control). In contrast, the activity of these antioxidants increased by 2.3- and 3-fold, respectively, in the case of *D. bardawil*, concentrations 0.012 and 0.025 µg·L^{-1} Irgarol 1051 as compared to the control, while it declined by 1.0-fold at 0.050 µg·L^{-1} Irgarol. These findings may validate the hypothesis of the study, which states that *C. salina* is more efficient than *D. bardawil* at dissociating exogenous H_2O_2. However, in the case of *C. salina* and *D. bardawil*, the maximal activity for these antioxidants were attained at concentrations of 0.50 µg·L^{-1} and 0.025 µg·L^{-1} of Irgarol 1051, respectively. Lipids, nucleic acids, and protein oxidation are strongly linked to the detrimental effects of ROS accumulation on cellular levels, which eventually result in changes to cell structure. Data demonstrating a concentration-dependent decrease in protein content in *C. vulgaris* cells in the presence of different Zn concentrations support the obtained results. The highest concentration of protein was found at high zinc levels, whereas lower concentrations showed a rise in protein content.

This is likely due to the upregulation of stress proteins, such as antioxidant enzymes, to enhance defense against toxicity or possibly indicate the maximal defense threshold [63].

There was a discernible rise in the overall antioxidant activity in both examined algae as compared to the control. A detailed analysis of the data revealed that antioxidant activity increased with rising Irgarol concentrations in both algae species, consistently exceeding the levels observed in their respective controls. The concentration of Irgarol at 0.50 $\mu g \cdot L^{-1}$ for *C. salina* and 0.025 $\mu g \cdot L^{-1}$ for *D. bardawil* showed the greatest increase in magnitude. At higher Irgarol concentrations, total antioxidant activity showed a slight decline in *D. bardawil* but remained elevated compared to the control in *C. salina*.

Belghith et al. [66] reported similar results, indicating that the microalgae halophilic *Dunaliella salina* treated with varying doses of Cd (II) demonstrated an increase in overall antioxidant capacity. The improvement of biological components engaged in defense mechanisms against Cd toxicity may be the cause of this increase. Additionally, Jobby et al. [67] showed that the activity of particular antioxidant enzymes was significantly reduced in *Chlorella vulgaris* cells exposed to different concentrations of Cr (VI).

The acquired results provide strong support for the findings of El-Agawany et al. [58], who indicated that an increase in the overall activity of antioxidants in *Spirulina platensis* is typically observed under any stress. Additionally, they noted that under mild stress, the antioxidants' high levels of activity prevented the peroxidation breakdown of proteins and lipids by scavenging reactive oxygen species (ROS). Additionally, Jungklang [68] noted that plants under stress frequently experience antioxidant stress due to an imbalance between the production of reactive oxygen species (ROS) and the antioxidants' capacity to quench them. According to reports, plants with high antioxidant levels are more resistant to oxidative damage because they are able to control the redox balance within their cells [69]. This is demonstrated by the fact that overall antioxidant levels, which include both enzymatic and non-enzymatic antioxidants, generally increased as stress levels increased, suggesting a cellular ability to withstand the stress. If the level of stress is not so severe as to exceed the concentration limit that could harm or kill the organism, then this conclusion can be supported. A similar outcome was also noted for *D. bardawil*, where a decrease in total antioxidant activity was reported at greater Irgarol 1051 concentrations. Actually, oxidative damage is promoted by environmental contaminants, particularly heavy metals, in two ways: either by raising ROS concentrations within cells or by decreasing the antioxidant capacity of cells [70].

3.4. Mapping Mass Concentration of Algae Along the Egyptian Mediterranean Sea

This section represents the potentiality of algal growth including *Chlorella salina* and *Dunaliella bardawil* along the Mediterranean seawater. Mapping the potential growth of *Chlorella salina* and *Dunaliella bardawil* along the Mediterranean Sea is crucial for environmental monitoring, aquaculture, pollution control, and climate change research. These algae play a key role in marine food webs and serve as indicators of water quality, nutrient levels, and ecosystem health. High algal growth areas, particularly near the Nile Delta, are vulnerable to eutrophication and pollution, making mapping essential for assessing the impact of nutrient runoff and toxic biocides like Irgarol 1051. Additionally, these algae support aquaculture, biofuel production, and pharmaceuticals, making their distribution important for economic sustainability. Understanding algal growth patterns also aids in carbon sequestration studies and helps policymakers develop strategies for marine conservation and coastal management. By integrating spatial analysis with environmental assessments, researchers can balance economic development and ecosystem preservation in Mediterranean coastal regions. The levels of Algae represented by chlorophyll-a mass concentration along the Egyptian Mediterranean coast ranged from 0.05 to 7.52 with a mean

value of 0.17 mg·m^{-3}. The highest values were recorded east and middle of the Egyptian coast (Figure 8). The mass concentration of chlorophyll-a along the shoreline is generally decreasing from east to west, fluctuating from 1 mg·m^{-3} at the eastern coast to 6.5 mg·m^{-3} at the middle Nile Delta coast with an obvious decrease moving westward reaching the lowest values at the west coast (<0.1 mg·m^{-3}). Low levels (<0.08 mg·m^{-3}) were reported in the coastal and deep water away from the shoreline.

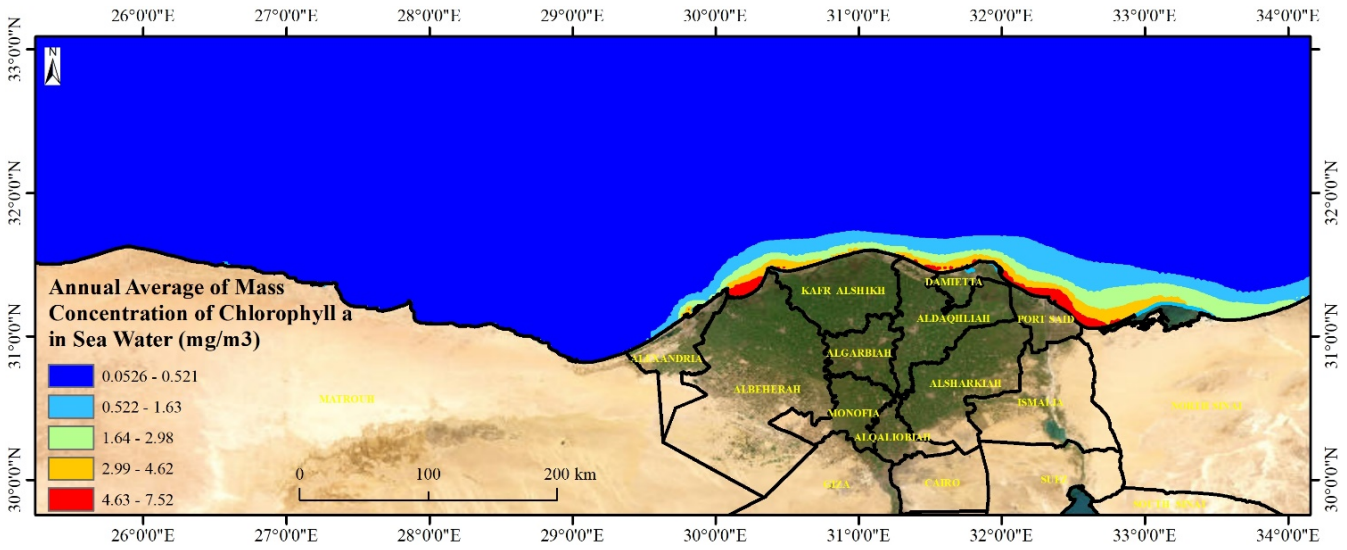

Figure 8. Mass average of chlorophyll–a (mg·m^{-3}) mapping along the Egyptian Mediterranean coast.

Levels of mass chlorophyll-a at the Mediterranean Sea governorates are decreasing with depth, showing the highest levels at the shoreline seawater (5 km from the shore) and the lowest levels at the deep water (200 km away from the shore) (Figure 9). This spatial trend was obvious in seawater in front of the Mediterranean Sea governorates. Further, the highest levels were observed in seawater of the Nile delta governorates: Port Said, Damietta, and Dakhalia shores reporting 6, 4.5, and 4 mg·m^{-3}, respectively (Figure 10). The lowest levels were observed along Matrouh and Alexandria shores reporting 0.075 and 0.8 mg·m^{-3}, respectively (Figure 11). The plenty of mass chlorophyll-a in front of the Egyptian northern governorates can be ordered as follows: Port Said > Damietta > Dakahlia > North Sinia > Kafr El-Sheikh > Alexandria > Matrouh.

The high chlorophyll-a concentration in seawater along the Delta governorates' shores of Egypt can be explained by several key factors such as nutrient enrichment, eutrophication, seasonal dynamics, and hydrological conditions. The Nile River delivers high levels of nitrogen and phosphorus from agricultural runoff and urban wastewater into the Mediterranean, boosting phytoplankton growth. These nutrients are essential for primary production, especially near river mouths [71]. Extensive human activities, including the use of fertilizers and discharges from urban areas, contribute to nutrient overloading, leading to eutrophication and algal blooms. Nutrient inputs vary seasonally, with river runoff peaking in autumn and winter, further supporting chlorophyll-a variability across different periods. Coastal plumes and limited water mixing near the southeastern Mediterranean coastline trap nutrients in localized areas, intensifying chlorophyll-a concentrations [72]. These interconnected processes, influenced by both natural and anthropogenic factors, make the coastal waters of Egypt's Delta region hotspots for high chlorophyll-a levels.

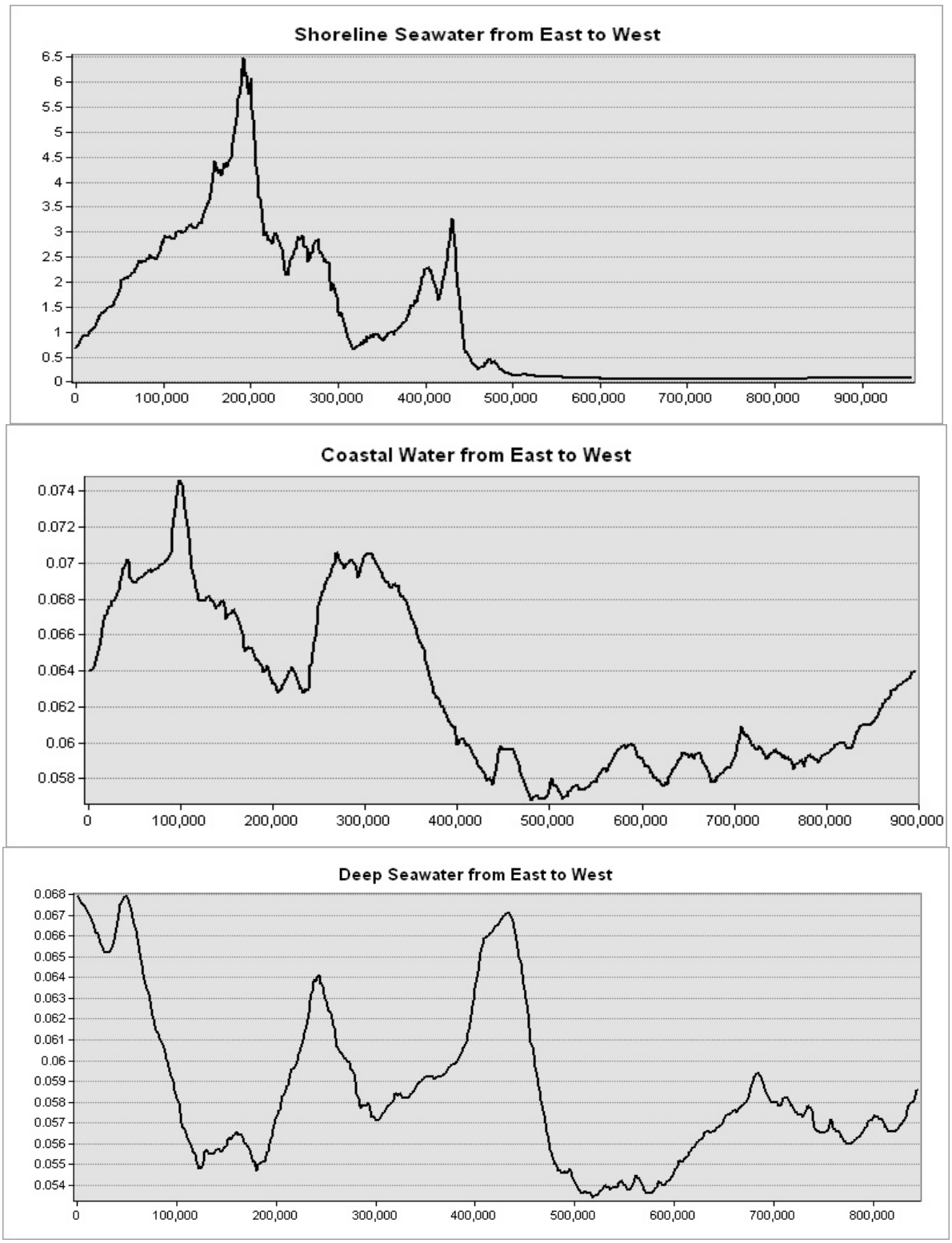

Figure 9. Mass chlorophyll-a ($mg \cdot m^{-3}$) along the Egyptian Mediterranean Sea from East to West.

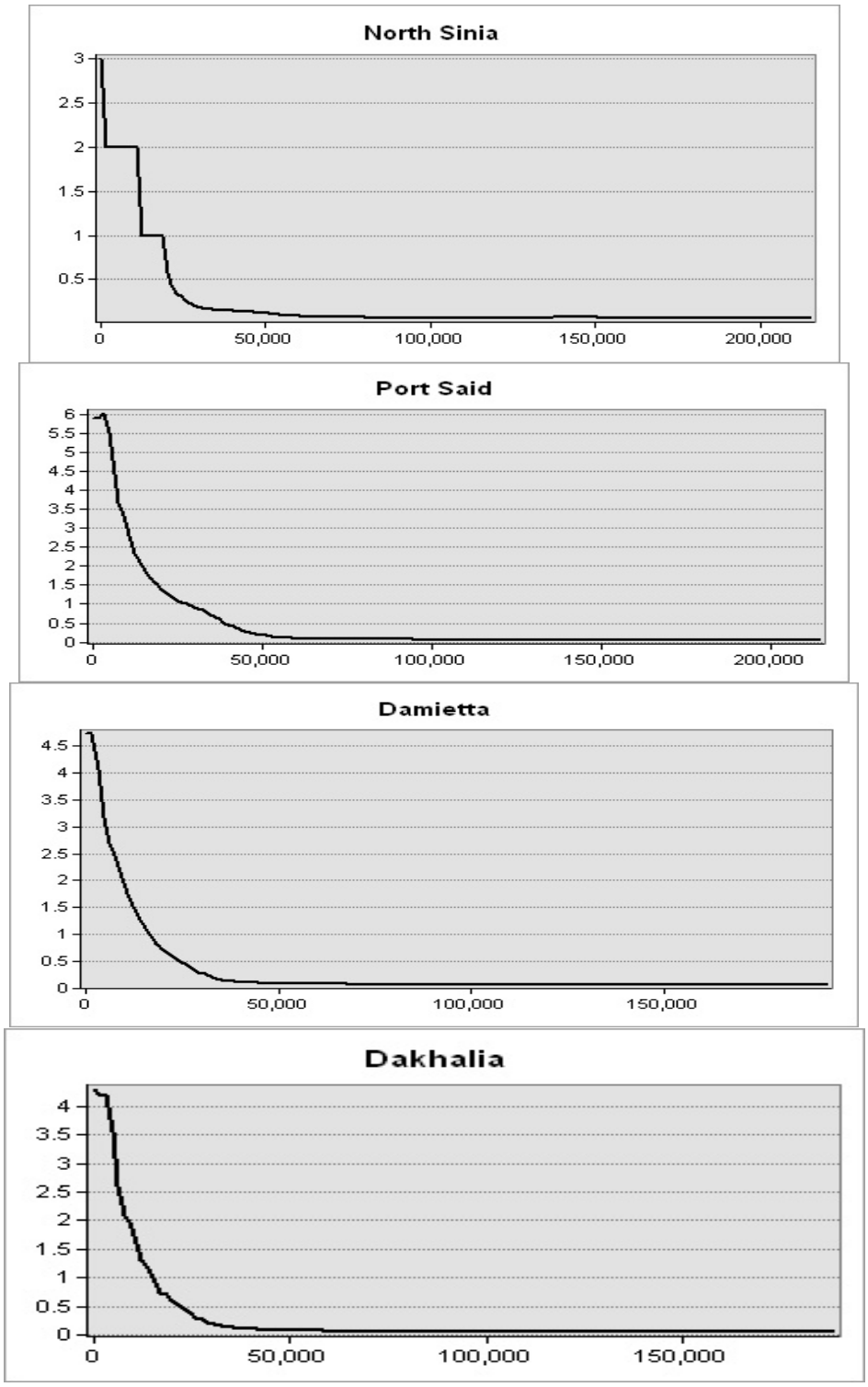

Figure 10. Mass chlorophyll-a ($mg \cdot m^{-3}$) at the Mediterranean Sea east and middle of the Nile delta governorates.

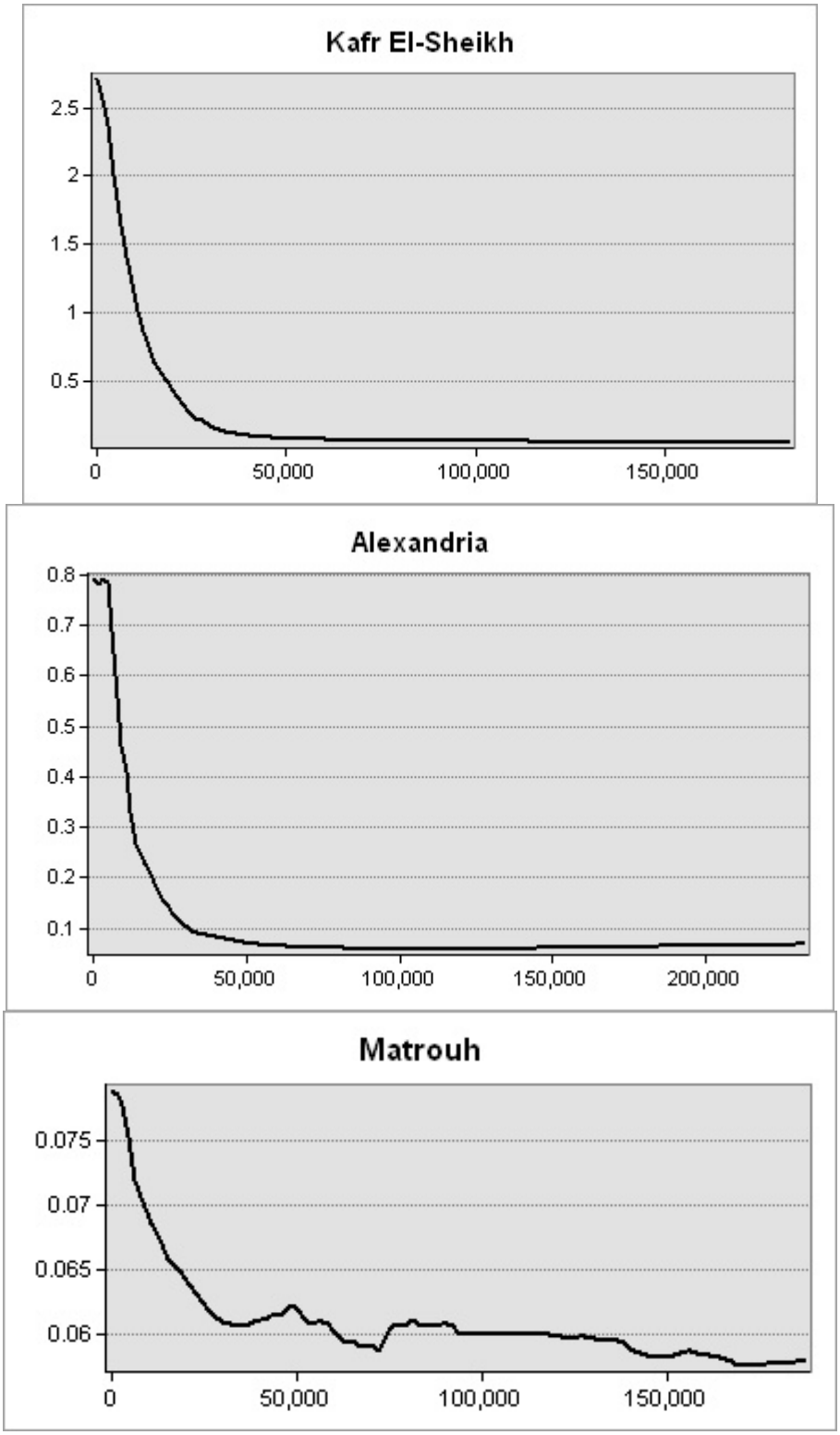

Figure 11. Mass chlorophyll-a ($mg \cdot m^{-3}$) at the Mediterranean Sea middle and west of the Nile delta governorates.

4. Conclusions

This study evaluated the harmful impacts of Irgarol 1051, a biocide antifouling compound, on the levels of some important metabolites such as protein profiles, I.R. spectroscopy of total cell constituents, and total antioxidant activities in two marine algal species; *Chlorella salina* and *Dunaliella bardawil*. It also tested the potential sites for algal

growth along the Egyptian Mediterranean coast using remote sensing and geostatistical analyses. The findings showed that Irgarol 1051 concentrations for *C. salina* were 0.25, 0.5, and 0.75 $\mu g \cdot L^{-1}$, whereas for *D. bardawil*, they were 0.012, 0.025, and 0.05 $\mu g \cdot L^{-1}$. There was a notable inhibition of algal growth rate for the two tested species at all the tested Irgarol concentrations, which corresponded to the increasing toxicity of this biocide.

The obtained I.R. spectra of the primary cell constituents revealed the disappearance of some peaks and the appearance of new ones, while others remained virtually unchanged. Protein synthesis in the stress adaptation mechanism of *C. salina* and *D. bardawil* after a time of stress demonstrated the presence of species-stressed proteins for a specific environmental stress factor (i.e., Irgarol compounds). The number of protein profile bands depends primarily on the species type and concentration of the stressed substance. The antifouling chemical Irgarol 1051 had a more negative impact on the protein profile in the wall-less alga *D. bardawil* than in the walled alga *C. salina*.

The activity of total antioxidants altered with various doses of Irgarol increased gradually, if at all, throughout the tests. Total antioxidant activity in both examined algae increased significantly when compared to the control group. A careful inspection of the outputs revealed that as Irgarol concentration increased, the antioxidant activity increased, which was higher in both algae than in the corresponding controls except at the highest concentration.

Spatial investigation indicated that the levels of mass chlorophyll-a at the Mediterranean Sea governorates are decreasing with depth showing the highest levels at the shoreline seawater and the lowest levels at the deep water. The highest levels were observed in seawater of the Nile delta governorates: Port Said, Damietta, and Dakhalia shores reporting 6, 4.5, and 4 $mg \cdot m^{-3}$, respectively. The lowest levels were observed along Matrouh and Alexandria shores reporting 0.075 and 0.8 $mg \cdot m^{-3}$, respectively. The high chlorophyll-a concentration in seawater along the Delta governorates' shores of Egypt can be explained by several key factors: nutrient enrichment and eutrophication, from the River Nile at Damietta and Rasheed branches.

The overall outcomes of this investigation show that Irgarol 1051 has the potential to have a negative influence on all the studied metabolites of the two algae species at environmentally relevant concentrations. Furthermore, this reinforces the importance of spatial analyses of algae in maximizing both economic and environmental benefits.

Environmental implication:

- The study reveals the toxic effects of Irgarol 1051 on marine algae species *Chlorella salina* and *Dunaliella bardawil*, which are crucial for the marine food web. The decline of these algae could lead to cascading effects on other marine species.
- The study also raises concerns about Irgarol 1051's potential for bioaccumulation and biomagnification, potentially causing higher concentrations in top predators and further harm.
- The spatial analysis reveals high algal growth areas near the Nile Delta along the Egyptian coast, potentially vulnerable to the effects of Irgarol 1051 due to nutrient runoff and eutrophication.
- The presence of a toxicant and increased antioxidant activity in the algae indicate stress, which is often used as a biomarker of environmental contamination, suggesting that Irgarol 1051 is inducing a physiological stress response in these organisms.

Future work:

- The study on Irgarol 1051, a biocide, focuses on its short-term effects on two algal species. It suggests that future research should explore the long-term, and chronic effects on these algae, including reproduction, genetic changes, and potential recovery.

- It also highlights the importance of investigating the effects on other marine organisms, such as other algae, zooplankton, fish, and benthic invertebrates, to assess the broader ecosystem risks.
- The study also highlights the potential synergistic effects of Irgarol 1051 in combination with other pollutants, such as heavy metals, pesticides, or other antifouling agents.
- The study emphasizes the need for the development of alternative antifoulants and the need for spatial modeling and risk assessment to minimize the environmental impact of Irgarol 1051. It also suggests the influence of eutrophication on the toxicity of Irgarol 1051 and the sensitivity of algae.
- The spatial analysis provided valuable insights into the algal distribution and potential Irgarol 1051 impact zones. Future studies should explore the use of advanced geospatial techniques, such as higher-resolution satellite data and machine learning for improved classification. Incorporating additional environmental factors like sea surface temperature and nutrient levels could enhance the assessment of eutrophication hotspots. Furthermore, hydrodynamic models may offer a better understanding of pollutant dispersion and its impact on coastal ecosystems.

Supplementary Materials: The following supporting information can be downloaded at https://www.mdpi.com/article/10.3390/jmse13040695/s1, Table S1: Effect of different concentrations of Irgarol 1051 on growth of *Chlorella salina* and *Dunaliella bardawil* cultured for 14 days; Table S2: Changes in protein profile in relation to the concentrations tested (0.25 $\mu g \cdot L^{-1}$ Irgarol 1051) in *Chlorella salina*; Table S3: Changes in protein profile in relation to the concentrations tested (0.50 $\mu g \cdot L^{-1}$ Irgarol 1051) in *Chlorella salina*; Table S4: Changes in protein profile in relation to the concentrations tested (0.75 $\mu g \cdot L^{-1}$ Irgarol 1051) in *Chlorella salina*; Table S5: Changes in protein profile in relation to the concentrations tested (0.012 $\mu g \cdot L^{-1}$ Irgarol 1051) in *Dunaliella bardawil*; Table S6: Changes in protein profile in relation to the concentrations tested (0.025 $\mu g \cdot L^{-1}$ Irgarol 1051) in *Dunaliella bardawil*; Table S7: Changes in protein profile in relation to the concentrations tested (0.050 $\mu g \cdot L^{-1}$ Irgarol 1051) in *Dunaliella bardawil*; Figure S1: Scanning of total band protein profile in *Chlorella salina* cells at the effect of different Irgarol 1051 concentrations (control and 0.25 $\mu g \cdot L^{-1}$, 0.50 $\mu g \cdot L^{-1}$, and 0.75 $\mu g \cdot L^{-1}$); Figure S2: Scanning of the total band protein profile of *Dunaliella bardawil* cells at the effect of different Irgarol 1051 concentrations (control and 0.012 $\mu g \cdot L^{-1}$, 0.025 $\mu g \cdot L^{-1}$, and 0.050 $\mu g \cdot L^{-1}$); Figure S3: Protein profile bands pattern of *Chlorella salina* and *Dunaliella bardawil* cells cultured at control conditions and at different Irgarol 1051 concentrations.

Author Contributions: Conceptualization, M.I.A.K. and A.M.E.-Z.; methodology, M.I.A.K. and A.M.E.-Z.; formal analysis, M.I.A.K. and A.M.E.-Z.; lab experiment, M.I.A.K.; spatial analyses, A.M.E.-Z.; investigation, M.I.A.K., A.M.E.-Z., A.S. and M.D.; writing—original draft preparation, M.I.A.K. and A.M.E.-Z.; writing—review and editing, M.I.A.K., A.M.E.-Z., A.S. and M.D. All authors have read and agreed to the published version of the manuscript.

Funding: This paper was supported by School of Agricultural, Forest, Food, and Environmental Sciences (SAFE), University of Basilicata, Via dell'Ateneo Lucano 10, 85100 Potenza, Italy.

Data Availability Statement: This article contains all of the data that were created and examined during the study.

Acknowledgments: Authors acknowledge Copernicus Marine (https://marine.copernicus.eu/) for providing marine data to the present study (Accessed data September 2024).

Conflicts of Interest: The authors declare no conflicts of interest.

References

1. Chambers, L.D.; Stokes, K.R.; Walsh, F.C.; Wood, R.J.K. Modern approaches to marine antifouling coatings. *Surf. Coat. Technol.* **2006**, *201*, 3642–3652.
2. Danouche, M.; El Ghachtouli, N.; El Baouchi, A.; El Arroussi, H. Heavy metals phycoremediation using tolerant green microalgae: Enzymatic and non-enzymatic antioxidant systems for the management of oxidative stress. *J. Environ. Chem. Eng.* **2020**, *8*, 104460.
3. Muller-Karanassos, C.; Arundel, W.; Lindeque, P.K.; Vance, T.; Turner, A.; Cole, M. Environmental concentrations of antifouling paint particles are toxic to sediment-dwelling invertebrates. *Environ. Pollut.* **2021**, *268*, 115754.
4. Research and Markets Ltd. Research and Markets-Market Research Reports-welcome. 2025. Available online: https://www.researchandmarkets.com/ (accessed on 27 March 2025).
5. Kulkarni, Y. Antifouling Coatings Market Size to Hit USD 22.68 bn by 2034. Available online: https://www.precedenceresearch.com/antifouling-coatings-market?utm_source (accessed on 25 October 2024).
6. Readman, J.W. Development, Occurance, and regulation Of Antifouling Paints Biocides. *Handb. Environ. Chem.* **2006**, *5*, 1–15.
7. Kaamoush, M. Metabolic Response of the Two Marine Unicellular Algae *Chlorella salina* and *Dunaliella bardawil* to Toxicity of the Antifouling Agent Irgarol 1051. *J. Environ. Prot.* **2018**, *9*, 895–911.
8. Yebra, D.M.; Kill, S.; Dam-Johansen, K. Antifouling technology past, present and future steps towards efficient and environmentally friendly antifouling coatings. *Prog. Org. Coat.* **2004**, *50*, 75–104.
9. EPA. *Environmental Problems from Antifouling Agents*; R &D Technical Report P215 EA; EPA: Bristol, UK, 1998.
10. Thomas, K.V.; McHugh, M.; Hilton, M.; Waldock, M. Increased persistence of antifouling paint biocides when associated with paint particles. *Environ. Pollut.* **2003**, *123*, 153–161. [CrossRef]
11. Kaamoush, M.; El-Agawany, N.; Omar, M.Y. Environmental toxicological evaluation (in vitro) of copper, zinc and cybutryne on the growth and amino acids content of the marine alga *Dunaliella salina*. *Egypt. J. Aquat. Res.* **2023**, *49*, 23–32. [CrossRef]
12. Alzieu, C. Environmental problems caused by TBT in France: Assessment, regulations, prospects. *Mar. Environ. Res.* **1991**, *32*, 7–17. [CrossRef]
13. Envans, S.M.; Leksono, T.; McKinnell, P.D. Tributyltin pollution: A diminishing problem following legislation limiting the use of TBT-based anti-fouling paints. *Mar. Pollut. Bull.* **1995**, *30*, 14.
14. Bryan, G.W.; Gibbs, P.E.; Burt, G.R.; Hummerstone, L.G. The Decline of the Gastropod Nucella Lapillus Around South-West England: Evidence for the Effect of Tributyltin from Antifouling Paints. *J. Mar. Biol. Assoc. United Kingd.* **1986**, *66*, 611–640. [CrossRef]
15. Lichtenthaler, H.; Buschmann, C.; Knapp, M. How to correctly determine the different chlorophyll fluorescence parameters and the chlorophyll fluorescence decrease ratio RFd of leaves with the PAM fluorometer. *Photosynthetica* **2005**, *43*, 379–393. [CrossRef]
16. Tsang, C.K.; Lau, P.S.; Tam, N.F.Y.; Wong, Y.S. Biodegradation capacity of tributyltin by two *Chlorella* species. *Environ. Pollut.* **1999**, *105*, 289–297. [CrossRef]
17. Scarlett, A.; Donkin, M.E.; Fileman, T.W.; Donkin, P. Occurrence of the marine antifouling agent Irgarol 1051 within the Plymouth Sound locality: Implication for the green microalga Enteromorpha intestinalis. *Mar. Pollut. Bull.* **1997**, *34*, 645–651. [CrossRef]
18. Berard, A.; Dorigo, U.; Mercier, I.; Becker-van Slooten, K.; Grandjean, D.; Leboulanger, C. Comparison of the ecotoxicological impact of the triazines Irgarol 1051 and atrazine on microalgal cultures and natural microalgal communities in Lake Geneva. *Chemosphere* **2003**, *53*, 935–944. [CrossRef]
19. Jung, S.M.; Bae, J.S.; Kang, S.G.; Son, J.S.; Jeon, J.H.; Lee, H.J.; Jeon, J.Y.; Sidharthan, M.; Ryu, S.H.; Shin, H.W. Acute toxicity of organic antifouling biocides to phytoplankton *Nitzschia pungens* and zooplankton *Artemia larvae*. *Mar. Pollut. Bull.* **2017**, *124*, 811–818. [CrossRef] [PubMed]
20. Muñoz, I.; Bueno, M.J.M.; Agüera, A.; Fernández-Alba, A.R. Environmental and human health risk assessment of organic micro-pollutants occurring in a Spanish marine fish farm. *Environ. Pollut.* **2009**, *158*, 1809–1816. [CrossRef]
21. Cima, F.; Varello, R. Effects of Exposure to Trade Antifouling Paints and Biocides on Larval Settlement and Metamorphosis of the Compound Ascidian *Botryllus schlosseri*. *J. Mar. Sci. Eng.* **2022**, *10*, 123. [CrossRef]
22. Ferreira, A.M.; Matos, J.M.; Silva, L.K.; Viana, J.L.M.; Freitas, M.S.D.; Júnior, O.P.A.; Franco, T.C.R.; Brit, N.M. Assessing the spatiotemporal occurrence and ecological risk of antifouling biocides in a Brazilian estuary. *Environ. Sci. Pollut. Res.* **2024**, *31*, 3572–3581. [CrossRef]
23. Zhang, A.Q.; Zhou, G.J.; Lam, M.H.W.; Leung, K.M.Y. Toxicities of the degraded mixture of Irgarol 1051 to marine organisms. *Chemosphere* **2019**, *225*, 565–573. [CrossRef]
24. International Coatings Ltd. Antifouling-Legislation.pdf. 2004. "Antifouling-Legislation.pdf". Available online: https://books.google.com.eg/books? (accessed on 27 March 2025).
25. Marine Environment Protection Committee (MEPC). 75, 16–20 November (Virtual Session). 2019. Available online: https://www.imo.org/en/MediaCentre/MeetingSummaries/Pages/MEPC-75th-session.aspx (accessed on 27 March 2025).
26. Bito, T.; Okumura, E.; Fujishima, M.; Watanabe, F. Potential of *Chlorella* as a Dietary Supplement to Promote Human Health. *Nutrients* **2020**, *12*, 2524. [CrossRef]

27. Aly, S.M.; ElBanna, N.I.; Fathi, M. *Chlorella* in aquaculture: Challenges, opportunities, and disease prevention for sustainable development. *Aquac. Int.* **2023**, *32*, 1559–1586. [CrossRef]
28. Pratiwi, D.Y. A mini review-effect of *Dunaliella salina* on growth and health of shrimps. *Int. J. Fish. Aquat. Stud.* **2020**, *8*, 317–319.
29. Boussiba, S.A.; Vonshak, Z. Cohen; Y. Avissar; A. Richmond. Lipid and biomass production by the halotolerant microalga. *Nannochloropsis salina. Biomass* **1987**, *12*, 37–48. [CrossRef]
30. Robert, R.L.G. Growth Measurements. Division Rate. In *Handbook of Physiological Methods, Culturing Methods and Growth Measurements*; Stein, R.J., Ed.; Cambridge University Press: Cambridge UK, 1979; Volume 29, p. 311.
31. Kansiz, M.; Heraud, P.; Wood, B.; Burden, f.; Beardall, J.; Mc Naughton, D. Fourier transform infrared micro spectroscopy and chemometrics as a tool for the discrimination of cyanobacterial strains. *Phytochemistry* **1999**, *52*, 407–417. [CrossRef]
32. Gianazza, E.; Wait, R.; Sozzi, A.; Regondi, S.; Saco, D.; Labra, M.; Agradi, E. Growth and protein profile changes in Lepidium sativum L. plantlets exposed to cadmium. *Environ. Exp. Bot.* **2007**, *59*, 179–187. [CrossRef]
33. Azizullah, A. Bio-assessment and remediation of arsenic (arsenite As-III) in water by Euglena gracilis. *J. Appl. Phycol.* **2019**, *31*, 423–433. [CrossRef]
34. Gatidou, G.; Kotrikla, A.; Rontogianni, V.; Thomaidis, N.S. Toxic effect of the antifouling biocide Irgarol 1051 and its principal metabolites on the green alga *Dunaliella tertiolecta*. In Proceedings of the 8th International Conference on Environmental Science and Technology, Lemnos Island, Greece, 8–10 September 2003.
35. Kaamoush, M.; El-Agwany, N. Comparison between the toxicity of Copper and Irgarol 1051 as two different generations of antifoulings on growth and essential metabolites of marine algae (*Dunaliella salina* as a case study). *Egypt. J. Aquat. Biol. Fish.* **2021**, *25*, 487–508. [CrossRef]
36. Buma, A.G.; Sjollema, S.B.; van de Poll, W.H.; Klamer, H.J.; Bakker, J.F. Impact of the antifouling agent Irgarol 1051 on marine phytoplankton species. *J. Sea Res.* **2009**, *61*, 133–139. [CrossRef]
37. Kaamoush, M. Impact of biofouling and antifouling compounds on marine environment and fish food chain. In Proceedings of the International Maritime Transport & Logistics Conference (MARLOG 7), Innovation in Ports "The Gateway to The Future", Alexandia, Egypt, 18–20 March 2018.
38. Naumann, D.; Lasch, P. Infrared spectroscopy in microbiology. In *Encyclopedia of Analytical Chemistry: Applications, Theory and Instrumentation*; Meyers, R.A., Ed.; Wiley: Hoboken, NJ, USA, 2015. [CrossRef]
39. Sackett, O.; Petrou, K.; Reedy, B.; Hill, R.; Doblin, M.; Beardall, J.; Ralph, P.; Heraud, P. Snapshot prediction of carbon productivity, carbon and protein content in at Southern Ocean diatom using FTIR spectroscopy. *ISME J. Adv.* **2015**, *10*, 416–426. [CrossRef]
40. Dumas, P.; Miller, L. The use of synchrotron infrared microspectroscopy in biological and biomedical investigations. *Vib. Spectrosc.* **2003**, *32*, 3–21. [CrossRef]
41. Dao, L.; Beardall, J.; Heraud, P. Characterization of Pb-induced changes and prediction of Pb exposure in microalgae using infrared spectroscopy. *Aquat. Toxicol.* **2017**, *188*, 33–42. [CrossRef]
42. Williams, D.H.; Feleming, I. *Spectroscopic Methods in Organic Chemistry*, 5th ed.; McGraw Hill International, Ltd.: London, UK, 1996.
43. Solovchenko, A. Physiological role of neutral lipid accumulation in eukaryotic microalgae under stresses. *Russ. J. Plant Physiol.* **2012**, *59*, 167–176. [CrossRef]
44. El-Agawany, N.; Kaamoush, M. Role of zinc as an essential microelement for algal growth and concerns about its potential environmental risks. *Environ. Sci. Pollut. Res.* **2022**, *30*, 71900–71911. [CrossRef]
45. Nelson, W.H. *Modern Technique for Rabid Microbiological Analysis*; VCH Publishers: New York, NY, USA, 1991.
46. El-Agawany, N.I. Metabolic Response of *Dunaliella tertiolecta* to Toxicity of Some Metals in Relation to Phosphorus Availability. Ph.D. Thesis, Botany and Microbiology Department, Faculty of Science, Alexandia University, Alexandia, Egypt, 2008.
47. Kaamoush, M. Metabolic Response of the Two Marine Algae *Dunaliella bardawil* and *Chlorella salina* to Toxicity of the Antifouling Agent IRGAROL 1051. Ph.D. Thesis, Botany and Microbiology Department, Faculty of Science, Alexandria University, Alexandia, Egypt, 2011.
48. Phong, W.N.; Show, P.L.; Le, C.F.; Tao, Y.; Chang, J.S.; Ling, T.C. Improving cell disruption efficiency to facilitate protein release from microalgae using chemical and mechanical integrated method. *Biochem. Eng. J.* **2018**, *135*, 83–90.
49. Mohy El-Din, S.M.; Abdel-Kareem, M.S. Effects of Copper and Cadmium on the Protein Profile and DNA Pattern of Marine Microalgae *Chlorella salina* and *Nannochloropsis salina*. *Environ. Process.* **2020**, *7*, 189–205. [CrossRef]
50. Hagemann, M.; Wittenburg, E. Salt-induces changes in the RNA and DNA content of cyanobacteria (blue-green algae) *Synechocystis aquatilis* and *Microcystis firma* in batch and turbidostate cultures. *Arch. Hydrobiol.* **1989**, *56* (Suppl. S82), 381–391.
51. Hagemann, M.; Erdmann, N.; Schiewer, U. Salt adaptation of the cyanobacterium *Microcystis firma* and *Synechocystis aquatilis* in turbidostate cultures, I. Steady state values. *Arch. Hydrobiol. Suppl.* **1989**, *82*, 425–435.
52. Hagemann, M.; Wolfel, L.; Krl Ulger, B. Alternation of protein synthesis in the cyanobacterium *Synechocystis* sp. PCC 6803 after salt shock. *J. Gen. Microbiol.* **1990**, *136*, 1393–1399.

53. Mohy El-Din, S.M.; Noaman, N.H.; Zaky, S.H. Effects of chloramphenicol, clofibric acid, acetyl salicylic acid, nonylphenol and bisphenol on the protein profile and ultrastructure of marine macroalgae *Pterocladia capillacea* and *Ulva lactuca*. *Egypt. J. Bot.* **2016**, *56*, 335–351. [CrossRef]
54. El Taher, A.M. Copper and Zinc Toxicity in Chlorella Vulgaris: Response of Growth; Some Metabolic and Antioxidants Activity. Master's Thesis, Faculty of Science, Alexandia University, Alexandia, Egypt, 2012.
55. Exss-Sonne, P.; Tolle, J.; Bader, K.P.; MichelK, P. The Idil a protein of *Synechocystis* sp functions in protecting the acceptor side of photosystem II under oxidative stress. *Photosynth Res.* **2000**, *63*, 145–157. [CrossRef]
56. Sinha, R.P.; Hader, D.P. Response of a rice field cyanobacteria *Anabaena* sp. To physiological stressors. *Environ. Exp. Bot.* **1996**, *36*, 147–155. [CrossRef]
57. Fulda, S.; Mikkat, S.; Schroder, W.; Hagemann, M. Isolation of salt—Induced periplasmic proteins from *synechocystis* sp. Strain pcc 6803. *Arch. Microbiol.* **1999**, *171*, 214–217. [CrossRef] [PubMed]
58. El-Agawany, N.; Mona Kaamoush, M.; El Salhin, H. Nutritional and toxicological importance of nickel, copper and zinc elements in *Spirulina platensis*. In Proceedings of the International Maritime and Logistics Conference "Marlog 12", Innovative Technologies for Ports and Logistics Towards a Sustainable Resilient Future", Alexandria, Egypt, 12–14 March 2023.
59. Salah El-Din, R.A. Contribution to the Biological and Phytochemical Studies of Marine Algal Vegetation on the Coast of Red-Sea and Suez-Canal (Egypt). Ph.D. Thesis, Botany Department, Faculty of Science, Al-Azhar University, Cairo, Egypt, 1994.
60. Ahmed, E.A.M. Impact of Tributyltin (TBT) on Metabolism of Some Marine Algae. Ph.D. Thesis, Faculty of Science, Alazhar University, Cairo, Egypt, 2010.
61. Gauthier, M.R.; Senhorinho, G.N.A.; Scott, J.A. Microalgae under environmental stress as a source of antioxidants. *Algal Res.* **2020**, *52*, 102104. [CrossRef]
62. Sathasivam, R.; Radhakrishnan, R.; Hashem, A.; Abd Allah, E.F. Microalgae metabolites: A rich source for food and medicine. *Saudi J. Biol. Sci.* **2019**, *26*, 709–722. [CrossRef]
63. Ajitha, V.; Sreevidya, C.P.; Sarasan, M.; Park, J.C.; Mohandas, A.; Singh, I.B.S.; Puthumana, J.; Lee, J. Effects of zinc and mercury on ROS-mediated oxidative stress-induced physiological impairments and antioxidant responses in the microalga *Chlorella vulgaris*. *Environ. Sci. Pollut. Res.* **2021**, *28*, 32475–32492. [CrossRef]
64. Knauert, S.; Knauer, K. The role of reactive oxygen species in copper toxicity to two fresh green algae. *J. Phycol.* **2008**, *44*, 311–319. [CrossRef]
65. Winterbourn, C.C. Superoxide dependent formation of hydroxyl radicals in the presence of iron salts is a feasible source of hydroxyl radicals in vivo. *Biochem. J. Lett.* **1982**, *205*, 461–463.
66. Belghith, T.; Athmouni, K.; Bellassoued, K.; El Feki, A.; Ayadi, H. Physiological and biochemical response of *Dunaliella salina* to cadmium pollution. *J. Appl. Phycol.* **2016**, *28*, 991–999. [CrossRef]
67. Jobby, R.; Jha, P.; Yadav, A.K.; Desai, N. Biosorption and biotransformation of hexavalent chromium [Cr (VI)]: A comprehensive review. *Chemosphere* **2018**, *207*, 255–266. [CrossRef]
68. Jungklang, J. Physiological and Biochemical Mechanisms of Salt Tolerance in *Sesbania rostrata Berm* and *Obem* and *Phaseolus vulgaris* L. Ph.D. Thesis, ECA Agricultural University, Techuba, Japan, 2005.
69. Bor, M.; Özdemir, F.; Türkan, I. The effect of salt stress on lipid peroxidation and antioxidants in leaves of sugar beet, *Beta vulgaris* L. and wild beet-*Beta maritime* L. *Plant. Sci.* **2003**, *164*, 77–84. [CrossRef]
70. Sies, H. Glutathione and its role in cellular functions. Free Radic. *Biol. Med.* **1999**, *27*, 916–921.
71. Mabrouk, M.; Jonoski, A.H.P.; Oude Essink, G.; Uhlenbrook, S. Eutrophication and nutrient transport dynamics in the Mediterranean's southeastern coastal zone. *Water* **2018**, *10*, 1690. [CrossRef]
72. Lazzari, P.; Solidoro, C.; Ibello, V.; Salon, S.; Teruzzi, A.; Beranger, K.; Colella, S.; Crise, A. Seasonal and inter-annual variability of plankton chlorophyll and primary production in the Mediterranean Sea: A modelling approach. *Biogeosciences* **2012**, *9*, 217–238.